DOI: 10.1002/chem.200500414

The Chemical Bond in Polyphosphides: Crystal Structures, the Electron Localization Function, and a New View of Aromaticity in P_4^{2-} and P_5^-

Florian Kraus and Nikolaus Korber*[a]

Abstract: The incongruent solvation of $M^I_4P_6$ species (M^I = K, Rb, Cs) in liquid ammonia leads to a broad variety of polyphosphides such as P_7^{3-}, P_{11}^{3-}, and the putatively aromatic P_4^{2-} and P_5^-, which we investigated by using NMR spectroscopy and single-crystal X-ray structure analysis. The structures of $Cs_2P_4{\cdot}2NH_3$, $(K@[18]crown\text{-}6)_3K_3(P_7)_2{\cdot}10NH_3$, $Rb_3P_7{\cdot}7NH_3$, and $(Rb@[18]crown\text{-}6)_3P_7{\cdot}6NH_3$ are discussed and compared. The electron localization function ELF is used in a comparison of the chemical bonding of various phosphorus species. The variances of the basin populations provide a well-established measure for electron delocalization and therefore aromaticity. While comparable variance is calculated for P_4^{2-} and P_5^- it is observed in the lone pairs rather than in the basin populations of the bonds as in the prototypical aromatic hydrocarbons such as benzene or the cyclopentadienide anion. For this behavior, the term "lone pair aromaticity" is proposed.

Keywords: aromaticity · ELF (electron localization function) · liquid ammonia · polyphosphides · structure elucidation

Introduction

Despite its problematic definition, aromaticity is a well-known concept in chemistry[1,2] and is best established for classic hydrocarbons such as benzene C_6H_6, the cyclopentadienide anion $C_5H_5^-$ (Cp^-), or the cyclobutadiene dianion $C_4H_4^{2-}$. In recent years, the concept of aromaticity and Hückel's rule has been expanded to some inorganic compounds of the main group elements such as the polyhedral boranes, S_2N_2, or S_4^{2+} which may also be readily explained by the Wade–Williams rules, the Zintl–Klemm–Busmann concept, or Parthé's valence-electron concentration rules.[3–12] If one takes the diagonal relationship between phosphorus and carbon into account—or the principle of isolobality—one would expect structural and topological homologies of their respective compounds. For phosphorus–phosphorus single bonds, examples of this homology are especially prominent, as expected. This can be seen in the relationship between the (cyclo)alkane series and the (cyclic) polyphosphane or polyphosphide series,[13–15] as well as in oligocyclic polyphosphides, for example, the heptaphosphanortricyclane anion P_7^{3-} (Figure 1) or the trishomocubane-shaped P_{11}^{3-} (Figure 1) ion with nortricyclane[16] C_7H_{10} and trishomocubane[17] $C_{11}H_{14}$ as their respective hydrocarbon analogues.

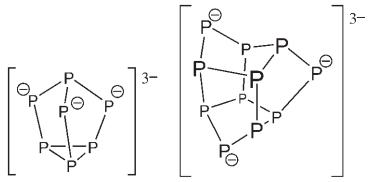

P_7^{3-} P_{11}^{3-}

Figure 1. Structures of the polyphosphide anions P_7^{3-} and P_{11}^{3-}.

As is to be expected, examples of phosphorus–phosphorus multiple or partial multiple bonds are less common, but they are found by invoking the P–C diagonal relationship again. Thus, the phosphorus analogue of benzene is P_6—an allotrope of phosphorus—which was discovered in the gaseous phase by mass spectrometry.[18] No structure could be assigned, however, but ab initio calculations show the benzvalene structure as a global minimum for anionic, neutral, and cationic hexaphosphorus compounds.[19–27] P_6 rings are found as building blocks of organometallic complexes such as $[\{(\eta^5\text{-}Cp^*)M\}_2(\mu,\eta^6\text{-}P_6)]$ (Figure 2) (Cp^* = pentamethylcyclopentadienyl, M = V,[28,29] Mo,[30] W[28]).

A class of extremely moisture- and air-sensitive compounds containing isolated P_6^{4-} rings (point group 6/*mmm*)

[a] F. Kraus, Prof. Dr. N. Korber
Institut für Anorganische Chemie der Universität Regensburg
Universitätsstrasse 31, 93053 Regensburg (Germany)
Fax.: (+49) 941-943-1812
E-mail: nikolaus.korber@chemie.uni-regensburg.de

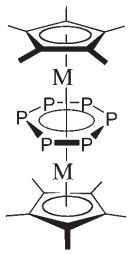

Figure 2. Structure of $[\{(\eta^5\text{-Cp*})M\}_2(\mu,\eta^6\text{-}P_6)]$ (M = V, Mo, W).

is found in the binary polyphosphides $M^I_4P_6$ (M^I = K,[31] Rb,[32,33] Cs;[33] Figure 3).

No solvates of these cyclohexaphosphides are known as yet, since P_6^{4-} is far too reactive and disproportionates in solution (glyme, ethylenediamine) to a complex mixture of polyphosphides and hydrogen(poly)phosphides. We have shown by ^{31}P NMR spectroscopy that several different products are obtained in the reaction of $M^I_4P_6$ with liquid, anhydrous ammonia.

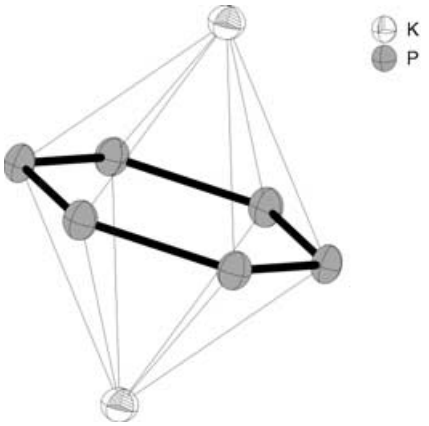

Figure 3. Structure of the $K_2P_6^{2-}$ unit in α-K_4P_6.[31]

A well-documented ion with partial multiple bond character is the 6π aromatic cyclopentaphosphide anion P_5^-[34–37] (Figure 4), the phosphorus analogue of Cp^-. P_5^- has been characterized by its chemical shift in ^{31}P NMR spectra.[34–37] P_5^- is also a well-known ligand in organometallic complexes which have been structurally analyzed by single-crystal X-ray diffractometry. Abundant examples include the ferrocene-like $[(\eta^5\text{-Cp*})M(\eta^5\text{-}P_5)]$ (M = Fe,[38] Ru, Os; Figure 4b) and the triple-decker $[\{(\eta^5\text{-Cp*})Cr\}_2(\mu,\eta^5\text{-}P_5)]$[39] (Figure 4c) by Scherer et al., and the fullerene-like $[\{Cp^*Fe(\eta^5{:}\eta^1{:}\eta^1{:}\eta^1{:}\eta^1\text{-}P_5)\}_{12}\{CuCl\}_{10}\{Cu_2Cl_3\}_5\text{-}\{Cu(CH_3CN)_2\}_5]$[40] by Scheer et al. However, neither a binary phosphide containing an isolated *cyclo*-P_5^- nor a corresponding solvate has been obtained in the crystalline state so far.

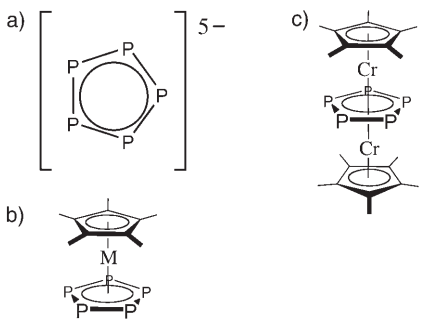

Figure 4. a) P_5^- and some organometallic complexes (b,c) containing it as a ligand.

Recently, the homologue of the 6π aromatic cyclobutadienyl dianion P_4^{2-} (point group D_{4h}) has been synthesized as an ammoniate by the reaction of diphosphane(4) and cesium in liquid ammonia. It may also be obtained as a crystalline by-product by reaction of white phosphorus in THF with cesium at −78 °C, followed by substitution of the THF by ammonia.[41] A very convenient way of producing $Cs_2P_4{\cdot}2\,NH_3$ has now been found, by ammonolysis of Cs_4P_6, while K_4P_6 and Rb_4P_6 yield a broad variety of (hydrogen)polyphosphides (see below). Another synthetic route to $Cs_2P_4{\cdot}2\,NH_3$ is by treatment with cesium of the dried, black, glass-like product of the reaction of diphosphane(4) with liquid ammonia, and condensation of ammonia on it. P_4^{2-} was known previously as a distorted ligand in organometallic complexes having D_{2h} or C_{2v} (kite-like) symmetry (Figure 5).[42–53] Butterfly-shaped P_4^{2-} (bicyclo[1.1.0.]tetraphosphide dianion) is obtained by reductive opening of P_4.[54–57] Four-membered planar phosphorus rings with D_{2h} symmetry can also be found in the skutterudite-type structure of CoP_3.[58,59]

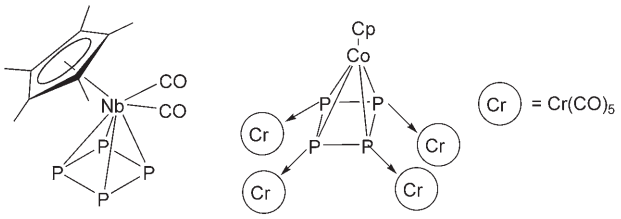

Figure 5. Drawings of organometallic complexes containing the P_4-ligand.

Here, we will focus on the P_6^{4-} phosphorus ring as an educt for a variety of reactions in liquid ammonia, and on the cyclotetraphosphide anion P_4^{2-}, its synthesis, its thermal stability, and its putative aromaticity viewed with the electron localization function ELF.

Results and Discussion

Ammonolysis of Cs_4P_6: When Cs_4P_6 reacts with liquid ammonia, $Cs_2P_4{\cdot}2\,NH_3$ is formed as a crystalline product, which we reported recently as the main product of the reaction of diphosphane(4) with cesium followed by solvation in liquid ammonia.[41] The formal reaction equation [Eq. (1)] could be established by NMR spectroscopy.

$$15\,Cs_4P_6 + 12\,NH_3 \rightarrow 21\,Cs_2P_4\cdot 2\,NH_3 + 6\,CsPH_2 + 12\,CsNH_2 \quad (1)$$

Structure of $Cs_2P_4{\cdot}2NH_3$: All the atoms reside on the common 4*e* position of space group $P2_1/a$. Two crystallographically inequivalent phosphorus atoms P(1) and P(2) are bonded to each other (P–P = 2.146(1) Å). By symmetry, two additional phosphorus atoms, P(1)#3 and P(2)#3, are generated with a bond length of 2.1484(9) Å to P(1). Thus, a four-membered, necessarily planar phosphorus ring with bond angles of 89.76(4)° and 90.24(4)° is formed (Figure 6). The bonds are shorter than the 2.219 Å P–P single bond in diphosphane(4) but significantly longer than the 2.034 Å P=P double bond in bis(2,4,6-tri-*tert*-butylphenyl)diphosphene.[20] In other homoatomic polyphosphorus anions (for example, P_7^{3-}, Figure 11 below), P–P bond lengths span a range from 2.12 Å to 2.29 Å, with the shorter bonds reaching from the triangular P-P-P base to the formally negatively charged, twofold bonded phosphorus atoms.[21] Thus, the P–P bond length in P_4^{2-} is not valid as a criterion of aromaticity. The cyclotetraphosphide anion P_4^{2-} is coordinated by eight symmetrically equivalent cesium cations; for Cs–P distances see the caption of Figure 6. The η^4-like coordinating cesium ions Cs(1) and Cs(1)#3 are 3.4118(6) Å above and below the P_4^{2-} plane and are shifted about 0.18 Å away from the center of the ring toward P(1). The coordination number of the cesium cation is nine (Figure 6b). As already mentioned, its coordination is η^4-like with a molecule of P_4^{2-} but also η^2-like with Cs–P distances of about 3.67 and 3.89 Å and two times η^1-like to two other, symmetrically equivalent cyclotetraphosphide anions with Cs–P distances of approximately 3.75 and 3.76 Å. The nitrogen atom N(1) of a molecule of ammonia of crystallization coordinates with the cesium cation with a distance of 3.264(3) Å. With N–N distances of more than 3.6 Å, N–H···N hydrogen bonding is not likely. The multitude of ionic and coordinative interactions present lead to the three-dimensional network structure of this compound (Figure 6c).

Further ways to synthesize $Cs_2P_4{\cdot}2NH_3$: Diphosphane(4) P_2H_4 reacts with liquid ammonia in the −78 °C to −40 °C range yielding a mixture of the ammonium polyphosphides $(NH_4)_2H_2P_{14}$, $(NH_4)_2P_{16}$, $(NH_4)_3P_{19}$, and $(NH_4)_3P_{21}$. Removal of NH_3 leads to a black solid consisting of a mixture of hydrogen-free polyphosphides that are richer in phosphorus.[60,61] Treatment of this black solid with various amounts of cesium in liquid ammonia below −40 °C leads to mixtures of $Cs_2P_4{\cdot}2NH_3$ and $Cs_3P_7{\cdot}3NH_3$ as the only crystalline products, which we have reported previously.[41,62] ^1H and $^{31}P\{^1H\}$ NMR spectroscopy provide evidence that the solution contains only P_4^{2-} and PH_2^-. Another method for the synthesis of $Cs_2P_4{\cdot}2NH_3$ is reaction of cesium with white phosphorus in THF at −78 °C and exchange of the solvent with liquid ammonia. $Cs_3P_7{\cdot}3NH_3$ is the main product; $Cs_2P_4{\cdot}2NH_3$ is only obtained as a by-product. ^{31}P NMR spectroscopy shows the only two phosphorus species present in solution are P_4^{2-} and PH_2^-.[41] In view of the chemical shift dependence of the cyclotetraphosphide anion on the counterion,[33,41] we searched for cesium–phosphorus coupling in the ^{133}Cs NMR of this solution at −40 °C (0.5 M CsBr in D_2O at 25 °C as external standard). We encountered a singlet of the cesium cation (chemical shift δ = 107.69; signal width ≈20 Hz). So, if Cs–P coupling is present, it should be smaller than 20 Hz.

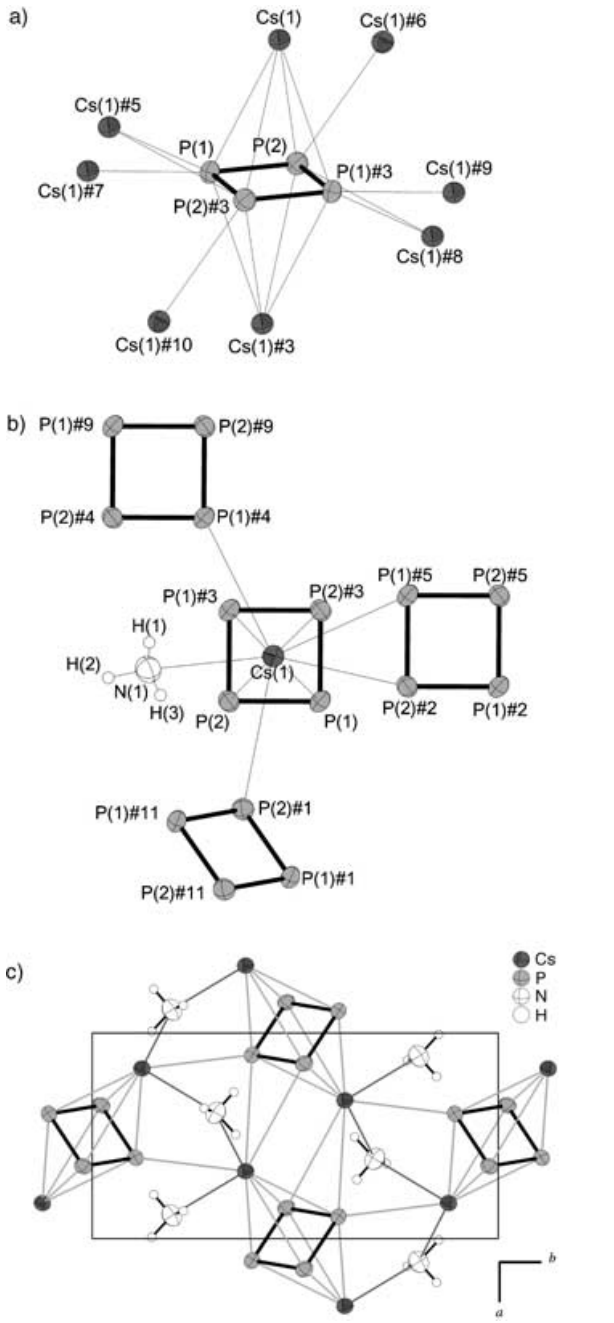

Figure 6. Projections of the coordination sphere of the P_4^{2-} anion (a) and of the cesium cation (b). c) Projection of the unit cell on the *ab* plane. Selected bond lengths [Å]: P(1)–P(2) 2.146(1), P(1)–P(2)#3 2.1484(9), P(1)–Cs(1) 3.7665(8), P(1)–Cs(1)#3 3.7023(7), P(1)–Cs(1)#5 3.8937(8), P(1)–Cs(1)#7 3.7529(8), P(2)–Cs(1) 3.7089(8), P(2)–Cs(1)#3 3.7651(7), P(2)–Cs(1)#6 3.7587(7), P(2)–Cs(1)#8 3.6742(9). Thermal ellipsoids are drawn at the 70% probability level. Symmetry transformations to generate equivalent atoms: #1: $x-1/2, -y+1/2, z$; #2: $x-1, y, z$; #3: $-x+1, -y, -z$; #4: $x, y, z+1$; #5: $-x, -y, -z$; #6: $x+1/2, -y+1/2, z$; #7: $x, y, z-1$; #8: $x+1, y, z$; #9: $-x+1, -y, -z+1$; #10: $-x+1/2, y-1/2, -z$; #11: $-x+1/2, y+1/2, -z$.

Thermal stability of the cyclotetraphosphide anion P_4^{2-}: After confirming the presence of P_4^{2-} in liquid ammonia in our initial report on the cyclotetraphosphide anion P_4^{2-} in $Cs_2P_4{\cdot}2NH_3$[41] the same fused NMR tube was kept at −40 °C for one year and five months, after which the ^{31}P NMR spectrum at −40 °C still showed the P_4^{2-} singlet (δ = 349 ppm), and additionally the PH_2^- triplet (δ = −270 ppm) and a small singlet at δ = −0.06 ppm which may stem from a phosphorus oxide species generated from the small amounts of moisture in the system. The ^1H NMR spectrum showed the presence of PH_2^- and amide NH_2^-. After this experiment, the fused NMR tube was stored for two months at room temperature. A subsequent ^{31}P NMR spectrum recorded at −40 °C still showed the presence of the species mentioned above, but with more amide and less PH_2^- present. The P_4^{2-} ion is stable up to at least +50 °C in liquid ammonia solution, as was again confirmed by ^{31}P NMR analysis at −40 °C after the fused NMR tube had been stored at +50 °C for one month. However, a small new signal at δ = −238 ppm was observed and no more PH_2^- could be detected in the ^{31}P and ^1H NMR spectra, but a large amide signal was present. Consequently, it may be concluded that PH_2^- deprotonated the ammonia and accumulated as monophosphane(3) (PH_3) in the gas phase in the fused NMR tube. Storage of the fused NMR tube at +100 °C unfortunately led to explosion of the tube. As we feared an explosion due to overpressure of the fused NMR tube in the NMR instrument, all our ^{31}P NMR spectra were recorded at −40 °C. Thus, a fast temperature-dependent equilibrium of P_4^{2-} with some other poly- or hydrogenpolyphosphides cannot be ruled out. However, we have not encountered any indication of such a phenomenon.

Slow removal of the ammonia of $Cs_2P_4{\cdot}2NH_3$ leads to an X-ray-amorphous yellow-gray product. After this powder had been kept in a sealed glass ampoule for three weeks at 500 °C, the X-ray powder diffraction pattern showed the presence of cesium phosphide(4/6) (Cs_4P_6) and an amorphous second component which may have been red phosphorus—a red substance like the latter covered the walls of the ampoule. This leads to the formal reaction equation [Eq. (2)].

$$4\,Cs_2P_4 \cdot 2\,NH_3 \rightarrow 2\,Cs_4P_6 + 4\,P + 8\,NH_3 \qquad (2)$$

Unfortunately, crystals have not yet been obtained from this reverse conproportionation.

Further reactions of Cs_4P_6 in liquid ammonia: In the reaction of cesium phosphide(4/6) with lithium in the presence of [18]crown-6 in liquid ammonia at −40 °C, the *catena*-trihydrogentriphosphide $P_3H_3^{2-}$ is formed as red, needle-shaped crystals of $(Cs@[18]crown\text{-}6)_2(P_3H_3){\cdot}7NH_3$, which will be reported elsewhere.

Ammonolysis of K_4P_6: When potassium phosphide(4/6) is dissolved in dry liquid ammonia, one observes a slightly blue solution turning green and finally yellow. $^{31}P\{^1H\}$ and ^1H NMR spectroscopy provide evidence that K_4P_6 disproportionates in liquid ammonia into P_5^-, P_4^{2-}, P_7^{3-}, P_{11}^{3-}, PH_2^-, and other poly- or hydrogenpolyphosphides we have not been able to identify yet. Up to now, P_{11}^{3-} has been accessible only by the solid-state route and to our knowledge it has never been generated in solution.

Storage of the yellow solution at −40 °C leads to the formation of transparent yellow crystals which redissolve at −78 °C, and which we have not yet been able to isolate for a single-crystal structure analysis.

Structure of $(K@[18]crown\text{-}6)_3K_3(P_7)_2{\cdot}10NH_3$: Using [18]crown-6 (1,4,7,10,13,16-hexaoxacyclooctadecane) for the generation of more stable crystals in this reaction, we could isolate $(K@[18]crown\text{-}6)_3K_3(P_7)_2{\cdot}10NH_3$ in the form of plate-shaped orange crystals as the only solid product. ^{31}P NMR shows the presence of P_7^{3-} and PH_2^- in the mother liquor. In the crystal structure, the phosphorus atoms of the heptaphosphanortricyclane anion P_7^{3-} reside on the common position (Wyckoff letter 2*i*) of the space group $P\bar{1}$. Selected bond lengths and angles of the P_7^{3-} cage are shown in Table 1; for a comparison with other P_7^{3-} cages, see Figure 11 (below) and Table 2. The experiment shows the shortest bonds to be those from the triangular base to the formally negatively charged phosphorus atoms,[63–65] which is confirmed here.

Table 1. Bond lengths and angles of the heptaphosphanortricyclane anion P_7^{3-} and its coordination to potassium ions.

P(1)–P(2)	2.1866(8)	P(1)–K(3)#5	3.5646(8)
P(1)–P(3)	2.1905(8)	P(3)–K(3)#5	3.3178(8)
P(1)–P(4)	2.1985(8)	P(3)–K(3)#3	3.3414(7)
P(2)–P(6)	2.1446(8)	P(4)–K(3)#5	3.4739(7)
P(3)–P(7)	2.1446(9)	K(2)–P(2)	3.2772(7)
P(4)–P(5)	2.1427(9)	K(2)–P(4)	3.5072(7)
P(5)–P(7)	2.2617(8)	K(2)–P(6)	3.6368(7)
P(5)–P(6)	2.2852(8)	K(2)–P(5)	3.8000(8)
P(6)–P(7)	2.3038(8)	K(4)–P(2)	3.2794(6)
		K(4)–P(3)	3.3305(7)
		K(4)–P(6)	3.4493(6)
		K(4)–P(7)	3.5177(7)
P(2)-P(1)-P(3)	101.30(3)	P(4)-P(5)-P(6)	105.30(3)
P(2)-P(1)-P(4)	102.70(3)	P(2)-P(6)-P(5)	105.52(3)
P(3)-P(1)-P(4)	102.10(3)	P(2)-P(6)-P(7)	105.57(3)
P(6)-P(2)-P(1)	98.36(3)	P(3)-P(7)-P(5)	105.04(3)
P(7)-P(3)-P(1)	99.20(3)	P(3)-P(7)-P(6)	103.63(3)
P(5)-P(4)-P(1)	98.03(3)	P(7)-P(5)-P(6)	60.88(2)
P(4)-P(5)-P(7)	106.11(3)	P(5)-P(6)-P(7)	59.06(2)
		P(5)-P(7)-P(6)	60.06(2)

The P_7^{3-} anion is coordinated by four potassium ions (Figure 7). Potassium ion K(2) coordinates in an η^4-like manner to the formally negatively charged phosphorus atoms P(2) and P(4) and the phosphorus atoms P(5) and P(6) of the triangular base of the cage. K(3)#5 is more than 4.6 Å away from the phosphorus atoms of the triangular base, which results in an η^3-like coordination to the apical phosphorus atom P(1) and the two formally negatively

Table 2. Comparison of the P_7^{3-} ions in the compounds under discussion.

	$(K@[18]crown\text{-}6)_3\text{-}K_3(P_7)_2\cdot 10\,NH_3$	$Rb_3P_7\cdot 7\,NH_3$	$(Rb@[18]crown\text{-}6)_3\text{-}P_7\cdot 6\,NH_3$
height h [Å]	3.0092(8)	2.987(2)	3.024(2)
mean distance a [Å]	2.284	2.281	2.291
mean distance b [Å]	2.144	2.137	2.146
mean distance c [Å]	2.192	2.182	2.198
ratio $Q = h/a$	1.318	1.309	1.319
angle γ [°]	98.53	98.17	98.90
angle δ [°]	102.03	102.45	101.71

charged atoms P(3) and P(4). K(3)#3 coordinates η^1-like at a distance of 3.3414(7) Å from P(3). Potassium ion K(4) resides on the special 1*f* position and coordinates η^4-like to the phosphorus atoms P(2), P(3), P(6), and P(7). The coordination sphere of the potassium ions is quite heterogeneous. K(1) is located on the special 1*e* position and is coordinated by a molecule of [18]crown-6. K(1) is also coordinated by a molecule of ammonia N(1) and its equivalent by symmetry, N(1)#1, yielding a coordination number of eight. Potassium ion K(2) is also coordinated by a molecule of [18]crown-6 which bonds to a molecule of ammonia N(1)#2 by N–H···O hydrogen bonding. Potassium ion K(3) coordi-

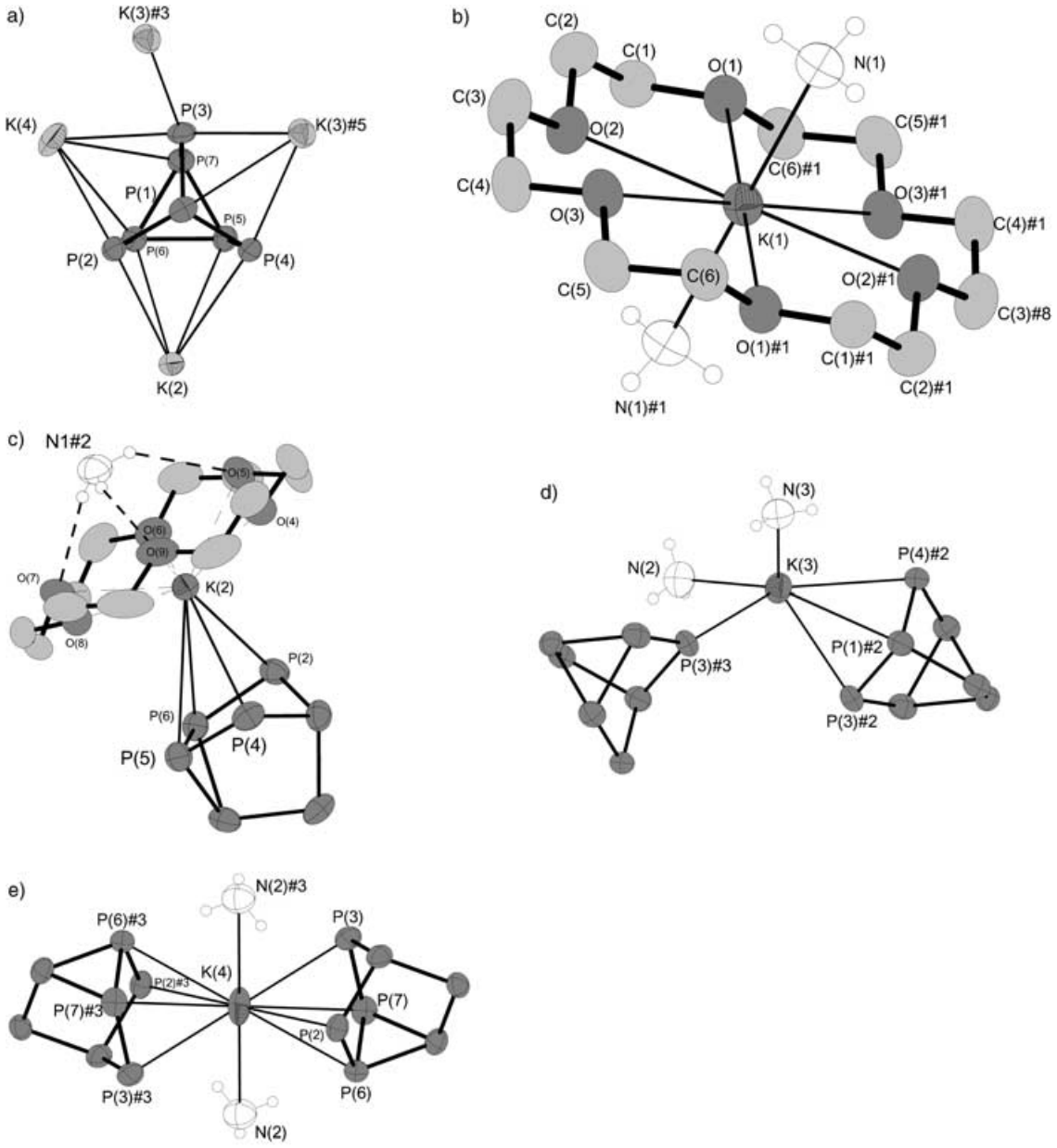

Figure 7. Projection of the coordination sphere of the P_7^{3-} ion (a) and the potassium ions K(1) (b), K(2) (c), K(3) (d), and K(4) (e). Hydrogen atoms of the crown ether molecules are omitted for clarity. Thermal ellipsoids are drawn at the 70% probability level. Symmetry transformations to generate equivalent atoms: #1: $-x+1, -y+1, -z$; #2: $x+1, y, z$; #3: $-x+3, -y, -z+1$; #5: $x-1, y, z$; #8: $-x+2, -y, -z$.

nates with two symmetrically equivalent P_7^{3-} cages in an η^1- and η^3-like fashion and to two molecules of ammonia N(2) and N(3). In addition to its η^4-like coordination to the phosphorus cage, potassium ion K(4) is bonded to two molecules of ammonia N(2) and N(2)#3 (Figure 7e).

Figure 8 shows a projection of the unit cell on the *bc* plane, indicating the relative arrangement of the structural elements in $(K@[18]crown\text{-}6)_3K_3(P_7)_2\cdot 10NH_3$ that have been discussed. For crystallographic details, see Table 3.

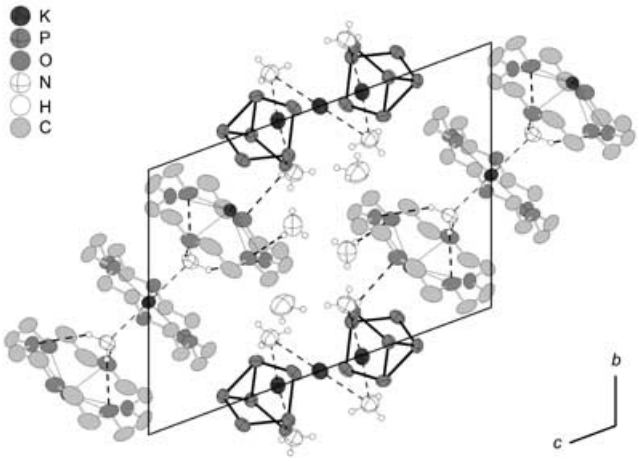

Figure 8. Projection of the unit cell on the *bc* plane. Hydrogen atoms of the crown ether molecules are omitted for clarity. Thermal ellipsoids are drawn at the 70% probability level.

Ammonolysis of Rb_4P_6: structure of $Rb_3P_7\cdot 7NH_3$: Rb_4P_6 reacts with liquid ammonia at −40 °C to yield yellow, plate-shaped crystals of $Rb_3P_7\cdot 7NH_3$ as the only solid product. $Rb_3P_7\cdot 7NH_3$ has also been synthesized previously in our group by congruent solvation of Rb_3P_7 in liquid ammonia.[66] In the crystal structure, all the atoms reside on the common 8*c* position of the space group *Pbca*. The P_7^{3-} ion shows typical P–P bond lengths in the range 2.130(2)–2.198(2) Å from the apical phosphorus atom to the formally negatively charged phosphorus atoms, 2.274(2)–2.290(2) Å from the latter to the trigonal base, and 2.179(2) to 2.189(2) Å in this basal plane. For a comparison of the heptaphosphanortricyclane anions discussed here, see Table 2 and Figure 11 below. The rubidium cation Rb(1) is coordinated by four molecules of ammonia at distances from 3.099(5) to 3.332(5) Å, and η^1- and η^4-like by two crystallographically inequivalent P_7^{3-}-cages at distances of 3.454(1) and within the range 3.500(1)–3.8(1) Å, respectively (Figure 9). Rb(2) also coordinates η^4-like to the heptaphosphanortricyclane anion with bond lengths of 3.538(1)–3.608(1) Å. Additionally, it is coordinated by five molecules of ammonia N(1), N(2), N(3), N(4), and N(6) at distances between 3.013(5) and 3.347(5) Å (Figure 9b). Finally, Rb(3) is coordinated by three molecules of ammonia at distances of 3.110(5)–3.361(5) Å and coordinates η^4-like to the phosphorus cage.

Table 3. Some crystallographic data of the structures presented.

	$(K@[18]crown\text{-}6)_3K_3(P_7)_2\cdot 10NH_3$	$Rb_3P_7\cdot 7NH_3$	$(Rb@[18]crown\text{-}6])_3P_7\cdot 6NH_3$	$Cs_2P_4\cdot 2NH_3$
empirical formula	$C_{18}H_{51}K_3N_5O_9P_7$	$H_{21}N_7P_7Rb_3$	$C_{36}H_{90}N_6O_{18}P_7Rb_3$	$H_6Cs_2N_2P_4$
molecular mass [g mol^{-1}]	815.73	592.44	1368.34	4.77
crystal system	triclinic	orthorhombic	triclinic	monoclinic
space group	$P\bar{1}$	*Pbca*	$P\bar{1}$	$P2_1/a$
a [Å]	10.3419(7)	17.802(1)	9.7111(9)	6.6580(7)
b [Å]	12.25(8)	17.894(1)	14.715(1)	12.579(1)
c [Å]	17.258(1)	13.398(1)	22.817(2)	6.7026(7)
α [°]	107.621(8)	90.0	100.29(1)	90.0
β [°]	104.491(8)	90.0	96.34(1)	106.18(1)
γ [°]	97.386(8)	90.0	90.19(1)	90.0
V [Å^3]	1964.6(2)	4267.9(5)	3187.6(5)	539.11(9)
Z	2	8	2	2
ρ_{calcd} [Mg m^{-3}]	1.397	1.844	1.419	2.611
T [K]	1(2)	1(2)	1(2)	1(2)
F(000) [e]	856	2288	1404	380
$\mu(MoK_\alpha)$ [mm^{-1}]	0.677	7.370	2.531	7.287
θ range [°]	2.59–28.08	2.24–27.89	2.09–25.95	3.16–25.96
measured/independent/observed ($I>2\sigma(I)$) reflections	34768/8819/7017	17743/4819/3813	22503/11499/6383	9093/1259/1189
R_{int}	0.0461	0.0522	0.0620	0.0575
h, *k*, *l* range	−13/13, −16/16, −22/22	−22/20, −23/23, −17/12	−11/11, −17/18, −27/27	−8/8, −16/16, −8/8
R(*F*) (all data)	0.0504	0.0592	0.0894	0.0206
$wR(F^2)$ (all data)	0.1091	0.1098	0.0900	0.0477
S	0.951	1.104	0.783	1.144
data/parameter/restraints	8819/427/6	4819/8/420	11499/682/3	1259/49/0
$(\Delta\sigma)_{max}$	0.001	0.001	0.002	0.000
$\Delta\rho_{max}$ [e Å^{-3}]	0.481	1.008	0.501	0.812
$\Delta\rho_{min}$ [e Å^{-3}]	−0.381	−0.842	−0.535	−0.504

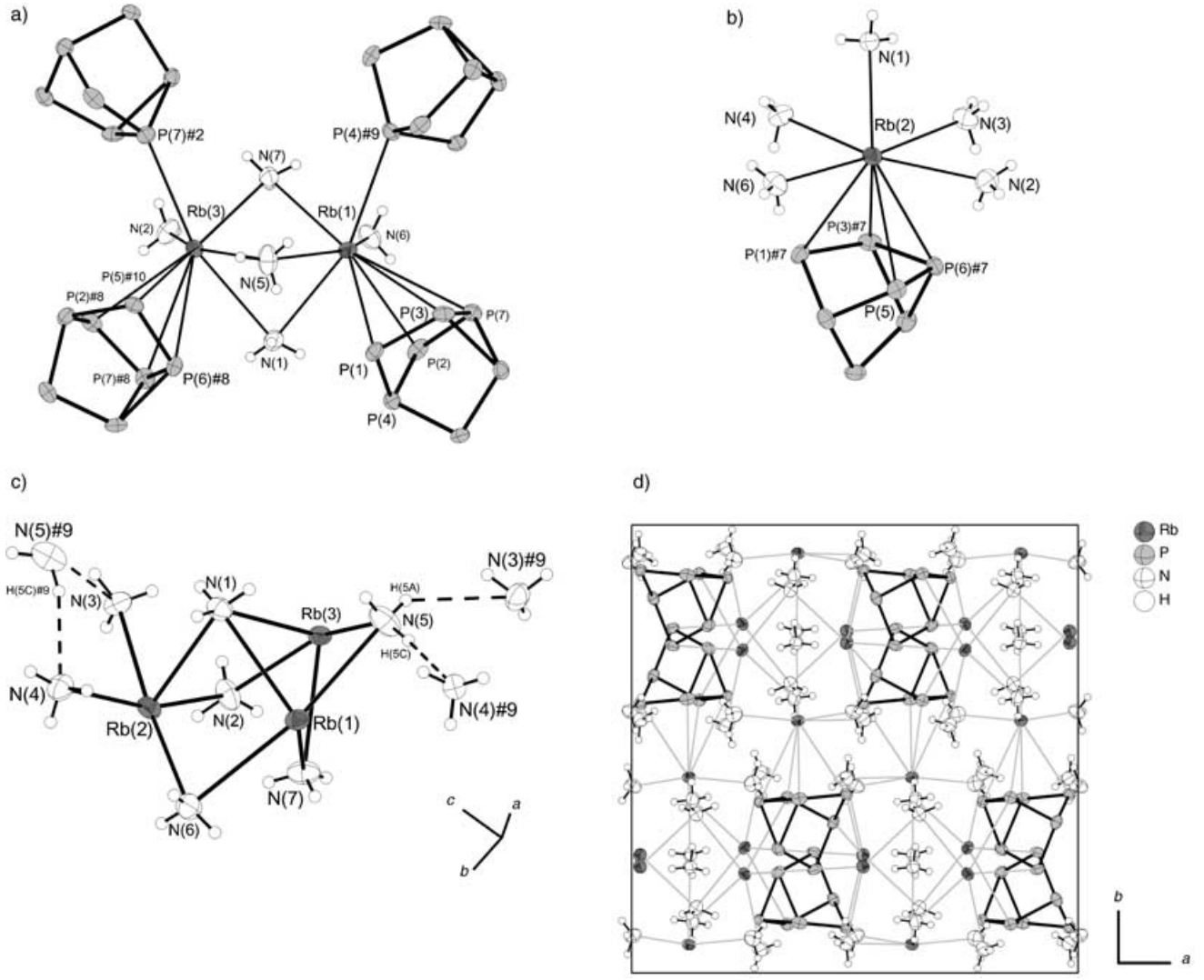

Figure 9. Projections of the coordination spheres of the rubidium cations Rb(1) and Rb(3) (a) and Rb(2) (b). c,d) Projection of one of the $[Rb_3(NH_3)_7]^{3+}$ clusters, which is interconnected via N–H···N hydrogen bonding (dashed bonds) forming one-dimensional infinite strands parallel to the *c* axis (c) and a projection of the unit cell on the *ab* plane (d). Thermal ellipsoids are drawn at the 70% probability level. Symmetry transformations to generate equivalent atoms: #2: $x + {}^1/_2, -y + {}^1/_2, -z$; #7: $-x, y + {}^1/_2, -z + {}^1/_2$; #8: $x + {}^1/_2, y, -z + {}^1/_2$; #9: $x, -y + {}^1/_2, z-{}^1/_2$; #10: $-x + {}^1/_2, y-{}^1/_2, z$.

The coordination of ammonia molecules to rubidium cations leads to the formation of rubidium–ammonia clusters, composition $[Rb_3(NH_3)_7]^{3+}$, in which N(1) acts as a μ^3-like bridging ligand; N(2), N(5), N(6), and N(7) bridge μ^2-like between the rubidium cations. These clusters are interconnected by N–H···N hydrogen bonding forming one-dimensionally infinite strands parallel to the *c* axis (D = donor, A = acceptor) (Figure 9): N(5)–H(5C)···N(4)#9 with D–H = 0.84(2) Å, H···A = 2.41(3) Å, D···A = 3.216(8) Å, ∢DHA = 163(6)°, N(5)-H5 A)···N(3)#9 with D–H = 0.84(2) Å, H···A = 2.77(4) Å, D···A = 3.470(8) Å, ∢DHA = 142(5)°. Since the P_7^{3-} ions are coordinated by rubidium cations, with Rb(1) and Rb(3) interconnecting crystallographically equivalent phosphorus cages, this also leads to the formation of one-dimensionally infinite strands parallel to the *c* axis (Figure 9c). Crystallographic details are in Table 3.

Structure of (Rb@[18]crown-6)$_3$P$_7$·6NH$_3$: Reaction of rubidium phosphide(4/6) with an excess of [18]crown-6 in liquid ammonia at −40 °C leads to thin yellow needle-shaped crystals of $(Rb@[18]crown\text{-}6)_3P_7{\cdot}6NH_3$ which are obtained as the only solid product. All atoms reside on the common 2*i* position of the space group $P\bar{1}$.

The P–P bond lengths in the basal plane of the P_7^{3-} anion of this structure are 2.274(2), 2.299(2), and 2.301(2) Å, respectively, those from the phosphorus atoms in the basal plane to the formally negatively charged ones are 2.145(2), 2.145(2), and 2.148(2) Å, and the bond lengths from the latter to the apical phosphorus atom are 2.188(2), 2.194(2). and 2.209(2) Å. For a comparison of the P_7^{3-} ions discussed here, see Table 2 and Figure 11 below. The cage anion is coordinated by three rubidium cations. Rb(1) and Rb(2) coordinate η^4-like at distances of 3.643(2)–3.743(2) Å to two phosphorus atoms of the basal plane and 3.340(1) to

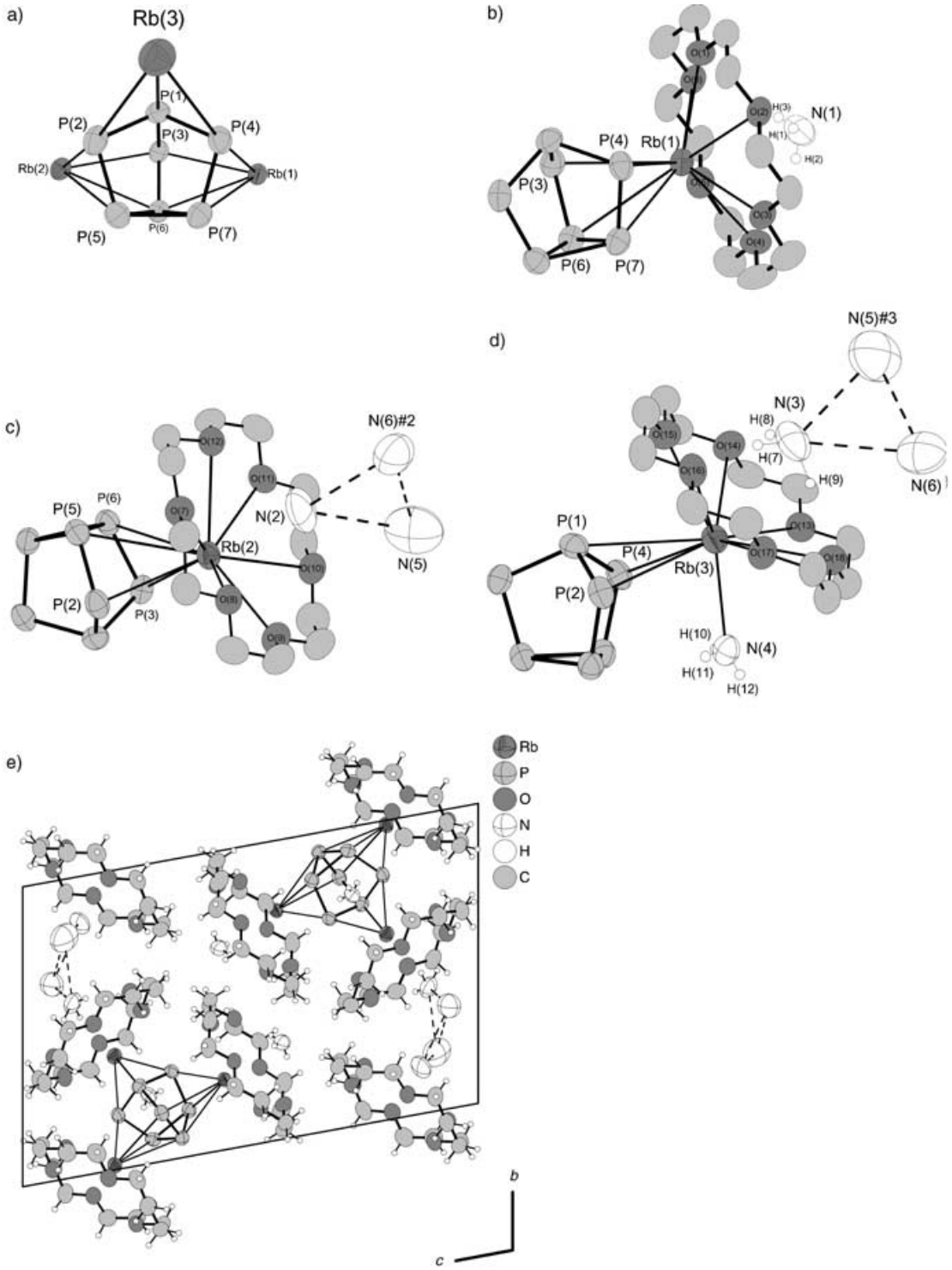

Figure 10. Foreshortened projection of the P_7^{3-} ion showing its coordination by rubidium cations (a), and projections of the coordination spheres of the rubidium ions Rb(1) (b), Rb(2) (c), and Rb(3) (d); hydrogen atoms of the crown ether molecules are omitted for clarity; projection of the unit cell on the *bc* plane (e). Thermal ellipsoids are drawn at the 70% probability level. Symmetry transformations to generate equivalent atoms: #2: $x-1, y+1, z$; #3: $x+1, y-1, z$.

3.510(1) Å to two formally negatively charged phosphorus atoms. Rb(3) coordinates η^3-like at distances of 3.790(2) Å to the apical phosphorus atom P(1) and 3.518(1) and 3.510(1) Å to the formally negatively charged atoms P(2) and P(4) (Figure 10). Each of the three rubidium cations is coordinated by a molecule of [18]crown-6 with Rb–O distances in the 3.008(3) to 3.364(4) Å range, leading to coordination numbers of ten for Rb(1) and Rb(2). Rb(3) also has

a coordination number of ten since it is additionally coordinated by the nitrogen atom N(4) of a molecule of ammonia of crystallization (Figure 10). In all, a neutral $[Rb([18]crown\text{-}6)(NH_3)]_2[Rb([18]crown\text{-}6)(NH_3)_2]P_7$ unit is generated by the coordinations mentioned. On the opposite side of each crown ether molecule a molecule of ammonia is bonded by N–H···O hydrogen bonding with O···H distances from 2.2 to 2.7 Å approximately. As the distance between the two molecules of ammonia N(5) and N(6)#2 is only about 3.36 Å, hydrogen bonding may be inferred, but we were not able to locate the hydrogen atoms on these atoms. N-H···N-hydrogen bonding from N(2) to N(5) and to N(6)#2 and from N(3) to N(6) and to N(5)#3 should also be present, with N···N distances being only around 3.3 Å (Figure 10). Thus, hydrogen bonding interconnects the $[Rb([18]crown\text{-}6)(NH_3)]_2[Rb([18]crown\text{-}6)(NH_3)_2]P_7$ units leading to the structure shown in Figure 10. Crystallographic details are in Table 3.

Further reactions of Rb_4P_6 in liquid ammonia: In the reaction of Rb_4P_6 with liquid ammonia in the presence of an excess of PPh_4Br, dark red needle-shaped crystals of $(PPh_4)_2(HP_7)\cdot 3\,NH_3$ are obtained. NMR spectrometric analysis of this solution shows only the presence of the tetraphenylphosphonium ion PPh_4^+, arguably due to the low solubility of $(PPh_4)_2(HP_7)\cdot 3\,NH_3$. This compound is also readily prepared by the reaction of K_3P_7 with a proton-charged ion-exchange resin in the presence of PPh_4Br in liquid ammonia.[67]

In the presence of lithium and [18]crown-6, Rb_4P_6 reacts in liquid ammonia at −40 °C to yield yellowish-green needle-shaped crystals of the hydrogen polyphosphide $(Rb@[18]crown\text{-}6)_2(P_3H_3)\cdot 7\,NH_3$, which will be reported elsewhere.

Comparison of the P_7^{3-} species obtained: To compare the P_7^{3-} anions presented here and to put them into context with other heptaphosphanortricyclane species in the literature, we use the height h and the mean bond lengths a, b, and c (Figure 11).[68] The ratio $Q = h/a$ may be used to quantify the ionicity of the P_7^{3-} cage. Q values in the range of about 1.30 to 1.36 denote ionic P_7^{3-} as found in all the species presented here, whereas values of 1.40 and higher show the presence of covalency as, for example, in $P_7(SiMe_3)_3$. In ionic Pn_7^{3-} cages (Pn = P, As, Sb), the angle γ is found to be smaller than the angle δ; the reverse is true for covalent species.[68,69] For the designation scheme used, see Figure 11.

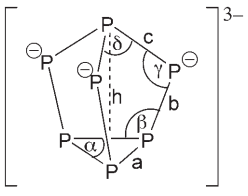

Figure 11. Structural drawing of the P_7^{3-} cage with designators of bond lengths and angles inscribed.[68]

The Q ratios are very similar, with values around 1.31 (Table 2). With values between 98° and 99°, the γ angles are smaller than the δ angles (approximately 102°). This fits well with the ionic description of these compounds.

The chemical shift and aromaticity of the cyclotetraphosphide anion P_4^{2-}: Examination of P_4^{2-} and other aromatic polyphosphides by NMR experiment is not trivial, since information cannot be gained on the molecular size and shape in these compounds. For aromatic polyphosphides one expects a singlet in the low-field region. Depending on its counterion, the concentration, and the temperature, we observe the chemical shift of the signal we assign to P_4^{2-} in ^{31}P NMR spectra at δ = 327.8 (K^+, −60 °C), 345.4 (Cs^+, −35 °C), and 343.0 ppm (Cs^+, −60 °C). The basis of our assignment of this chemical shift to P_4^{2-} rests, first, on the plausibility of a twofold negatively charged aromatic system showing a low-field singlet with a chemical shift that is less than the chemical shift of the aromatic P_5^-, which is about 468 in the ^{31}P NMR spectrum.[34–37] Second, there was good agreement between the chemical shift of P_4^{2-}, found by quantum-chemical calculations (δ = 359.6 ppm) at the HF/aug-cc-pVTZ level of theory, with the observed chemical shift of approximately 345.[41] A treatment within the HF method is only permitted since the CI coefficient of the RHF wavefunction is 0.972 in calculations at the [22,16]-CAS level for P_4^{2-}; for calculations of the chemical shift on the HF level of other tetrapnictogen dianions, the weight of the RHF wavefunction in a multiconfigurational approach needs to be evaluated first.[70]

Based on the NMR experiment these findings substantiate the aromaticity of P_4^{2-}.

Furthermore, P_4^{2-} has the same set of π molecular orbitals as the prototypical aromatic species such as benzene or the cyclopentadienide anion.[41]

To gain further insight into the chemical bonding and the aromaticity in polyphosphides such as P_4^{2-} and P_5^-, we used the electron localization function ELF. Within its model it has been shown that the degree of delocalization of electrons can be calculated and attributed to the aromaticity in compounds such as benzene, the cyclopentadienide anion, and aromatic, heteroatom-substituted, five-membered rings.[71,72]

ELF calculations: With calculations of the electron localization function (ELF)[73,74] and a population analysis of the resulting ELF basins including their population variances, we tried to gain a deeper understanding of the chemical bonds, lone pairs, and bond orders in polyphosphides such as P_7^{3-}, P_{11}^{3-}, in the aromatic polyphosphides P_4^{2-} and P_5^-, and in white phosphorus P_4. As a standard phosphorus–phosphorus single bond we used the central P–P bond in the known but not yet isolated hexaphosphane(8) $(H_2P)_2P\text{–}P(PH_2)_2$ (Figure 12) and compared its disynaptic valence basin population (denoted $V(P,P)$), its variance, and standard deviation with the phosphorus–phosphorus bonds of the polyphosphides mentioned. P_6H_8 seems to be a suitable choice for a standard P–P single bond in polyphosphorus compounds, as the two central phosphorus atoms are connected to two

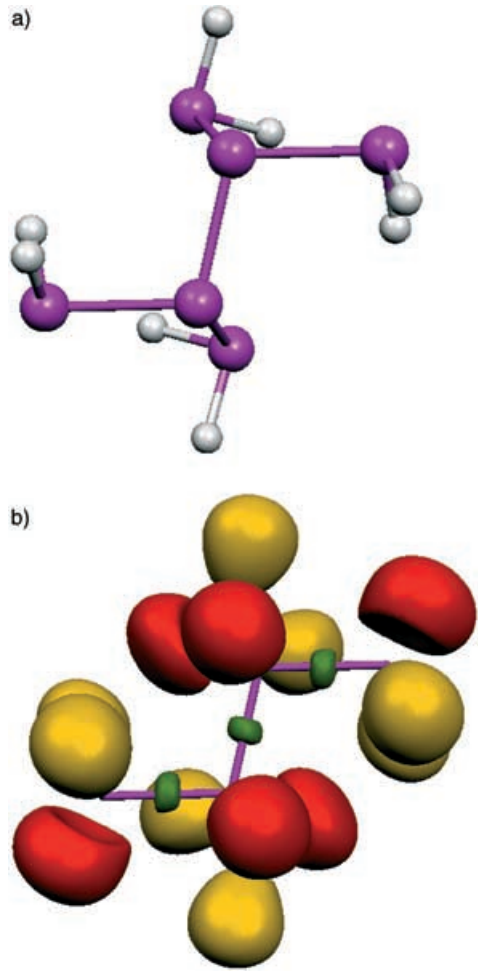

Figure 12. Projection of the structure (a) and the ELF of a molecule of P_6H_8 with $\eta(r) = 0.78$ (b). Core basins are omitted, monosynaptic valence basins are color-coded red, disynaptic valence basins green, and protonated disynaptic valence basins yellow.

other phosphorus atoms each and not to hydrogen atoms as in P_2H_4. The lone pairs, that is, the monosynaptic valence basins on the two central phosphorus atoms of P_6H_8 (denoted $V(P)$), are also used as a standard for comparison of the monosynaptic valence basins of the other polyphosphides.

In the population analysis of P_6H_8 (Table 4), $C(P)$ denotes the core basin of phosphorus; its population (in electrons, e) is close to 10 e, as expected. The population of the monosynaptic valence basin $V(P)$ is 2.14, and is thus larger than 2 with a variance σ^2 close to 1. The disynaptic valence basin population (1.89 e) is smaller than 2 with a variance of 1.07.

Table 4. Population in electrons, population variance, and standard deviations of the ELF basins of P_6H_8.

Basin[a]	Population	σ^2	σ
$C(P)$	10.04	0.48	0.69
$V(P)$	2.14	0.99	0.99
$V(P,P)$	1.89	1.07	1.03

[a] $C(P)$ is the mean core basin, $V(P)$ is the mean monosynaptic valence basin and $V(P,P)$ is the disynaptic valence basin of the central phosphorus atoms.

Table 5 contains the population analysis for the heptaphosphanortricyclane anion P_7^{3-} (Figure 13). In comparison with P_6H_8, the monosynaptic valence basins on the three basal phosphorus atoms are 1.07-fold more populated (2.30 e) with a 1.01-fold higher variance (1.00) as in hexaphosphane(8). Thus, the basal lone pairs in P_7^{3-} are very similar to the lone pairs on the central phosphorus atoms in P_6H_8. The two monosynaptic valence basins on a formally negative-charged phosphorus atom show a population of 1.98 e with a variance of 0.96, being 0.93-fold less populated with a lower variance than in our reference lone pair. The monosynaptic valence basin on the apical phosphorus atom

Table 5. Population in electrons, population variance, and standard deviations of the ELF basins of P_7^{3-}, and comparison with hexaphosphane(8).

Basin[a]	Population	σ^2	σ
$C(P)$	10.06	0.43	0.66
$V(P_{basal})$	2.30	1.00	1.00
$V(P^{\theta})$	1.98	0.96	0.98
$V(P_{apical})$	2.13	0.93	0.96
$V(P_{b.}, P_{b.})$	1.71	1.00	1.00
$V(P_{b.}, P^{\theta})$	1.94	1.08	1.04
$V(P^{\theta},P_{a.})$	1.84	1.03	1.01
scaled $V(P_{b.})$	1.07	1.01	1.01
scaled $V(P^{\theta})$	0.93	0.97	0.98
scaled $V(P_{a.})$	1.00	0.94	0.97
scaled $V(P_{b.}, P_{b.})$	0.90	0.93	0.97
scaled $V(P_{b.}, P^{\theta})$	1.03	1.01	1.01
scaled $V(P^{\theta}, P_{a.})$	0.97	0.96	0.98

[a] $C(P)$ is the mean core basin of the phosphorus atoms, $V(P_{basal})$ or $V(P_{b.})$ denotes the mean monosynaptic valence basins of the three basal phosphorus atoms, $V(P^{\theta})$ is the mean monosynaptic valence basin of the three formally negatively charged P atoms, $V(P_{apical})$ or $V(P_{a.})$ is the monosynaptic valence basin of the apical phosphorus atom. $V(P_{b.}, P_{b.})$, $V(P_{b.}, P^{\theta})$, and $V(P^{\theta}, P_{a.})$ are the corresponding mean disynaptic valence basins. "Scaled" refers to values obtained through division by the corresponding P_6H_8 values.

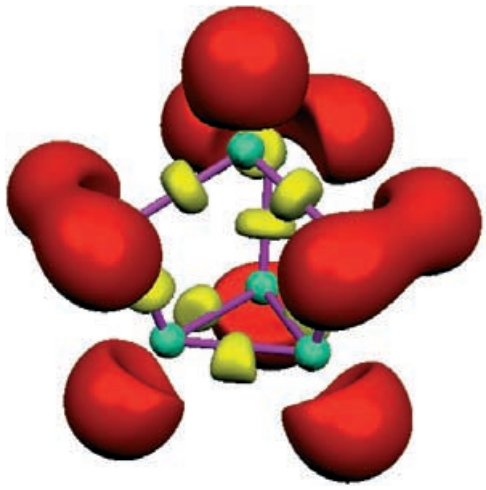

Figure 13. Projection of the ELF of the P_7^{3-} ion with $\eta(r) = 0.85$. Core basins are color-coded turquoise, monosynaptic valence basins red, and disynaptic valence basins yellow.

shows the same population as the one in the reference species with a slightly smaller variance. The basal phosphorus–phosphorus bonds are 0.90-fold less populated and have a lower variance than the reference P–P bond. The disynaptic valence basin between a basal and a formally negative-charged phosphorus atom is 1.03-fold more populated; the variance is 1.01-fold higher than in the reference. The P–P bond from the apical P atom to a formally negative-charged one is 0.97 times the population of P_6H_8 with a 0.96-fold variance.

Quite similar results are obtained for the trishomocubane-shaped P_{11}^{3-} (Figure 14). All the populations of the mono- and disynaptic valence basins and all its variances are very similar to the corresponding ones in the reference compound (Table 6). Consequently, it can be concluded that the chemical bonds and the lone pairs in the two polyphosphides P_7^{3-} and P_{11}^{3-} are not very different from those in our phosphane model.

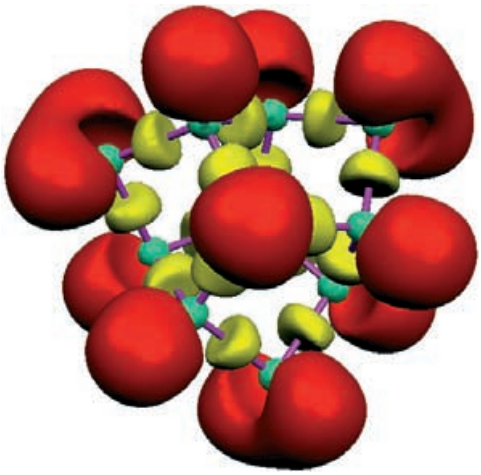

Figure 14. Projection of the ELF of the P_{11}^{3-} anion viewed along the C_3 axis with $\eta(r) = 0.78$. Core basins are color-coded turquoise, monosynaptic valence basins red, and disynaptic valence basins yellow.

Table 6. Population in electrons, population variance, and standard deviations of the ELF basins of P_{11}^{3-} and comparison with hexaphosphane(8).

Basin[a]	Population	σ^2	σ
$C(P)$	10.06	0.43	0.66
$V(P)$	2.09	0.89	0.94
$V(P^{\theta})$	1.99	0.96	0.98
$V(P_{apical})$	2.15	0.92	0.96
$V(P,P)$	1.89	1.02	1.01
$V(P, P^{\theta})$	1.89	1.05	1.02
$V(P, P_a)$	1.89	1.02	1.01
scaled $V(P)$	0.98	0.90	0.95
scaled $V(P^{\theta})$	0.93	0.97	0.98
scaled $V(P_a)$	1.00	0.93	0.96
scaled $V(P, P)$	1.00	0.95	0.97
scaled $V(P, P^{\theta})$	1.00	0.98	0.99
scaled $V(P, P_a)$	1.00	0.95	0.97

[a] $C(P)$ is the mean core basin of the phosphorus atoms, $V(P)$ denotes the mean monosynaptic valence basins of the six threefold bound phosphorus atoms, $V(P^{\theta})$ is the mean monosynaptic valence basin of the three formally negatively charged P atoms, and $V(P_{apical})$ or $V(P_a)$ is the mean monosynaptic valence basin of the two apical phosphorus atoms. $V(P, P)$, $V(P, P^{\theta})$, and $V(P, P_a)$ are the corresponding mean disynaptic valence basins. "Scaled" refers to values obtained through division by the corresponding P_6H_8 values.

A comparison of white phosphorus (Figure 15) with P_6H_8 shows only small differences (Table 7), too. The monosynaptic valence basins of P_4 are 1.18-fold more populated and the variance is 1.12-fold higher, and therefore the disynaptic valence basin is 0.87-fold less populated with a 0.93-fold lower variance than hexaphosphane(8), which may indicate the ease of bond cleavage in white phosphorus.

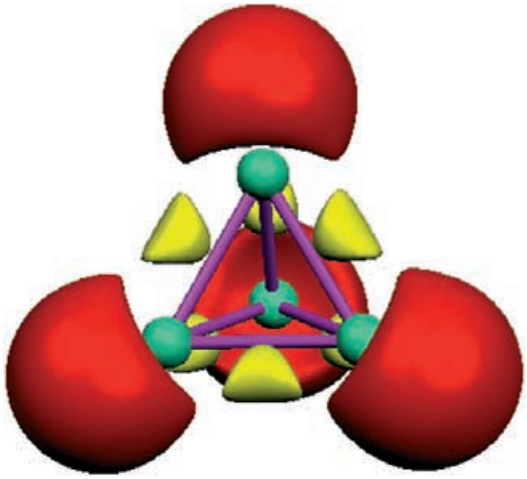

Figure 15. Projection of the ELF of a molecule of P_4 with $\eta(r) = 0.85$. Core basins are color-coded turquoise, monosynaptic valence basins red, and disynaptic valence basins yellow.

Table 7. Population in electrons, population variance, and standard deviations of the ELF basins of P_4 and comparison with hexaphosphane(8).

Basin[a]	Population	σ^2	σ
$C(P)$	10.02	0.44	0.66
$V(P)$	2.52	1.11	1.05
$V(P, P)$	1.64	0.99	0.99
scaled $V(P)$	1.18	1.12	1.16
scaled $V(P, P)$	0.87	0.93	0.96

[a] $C(P)$ is the mean core basin of the phosphorus atoms, and $V(P)$ denotes the mean monosynaptic valence basin. $V(P, P)$ is the mean disynaptic valence basin. "Scaled" refers to values obtained through division by the corresponding P_6H_8 values.

In the putatively aromatic polyphosphides P_4^{2-} and P_5^{-} the situation is strikingly different (Figure 16). Comparing their aromaticity with classic aromatic hydrocarbons such as benzene, one expects a large population of the disynaptic valence basins with a high variance indicating the delocalization of the electrons;[71,72] for example, for benzene the population of the C–C disynaptic valence basin is 2.80 e (close to 3) with a variance of 1.32. In P_4^{2-}, the population of the disynaptic valence P–P basin is only 2.10 e with a variance of only 1.13, thus being only 1.11 times more populated with a 1.06-fold higher variance as in the hexaphosphane(8) mol-

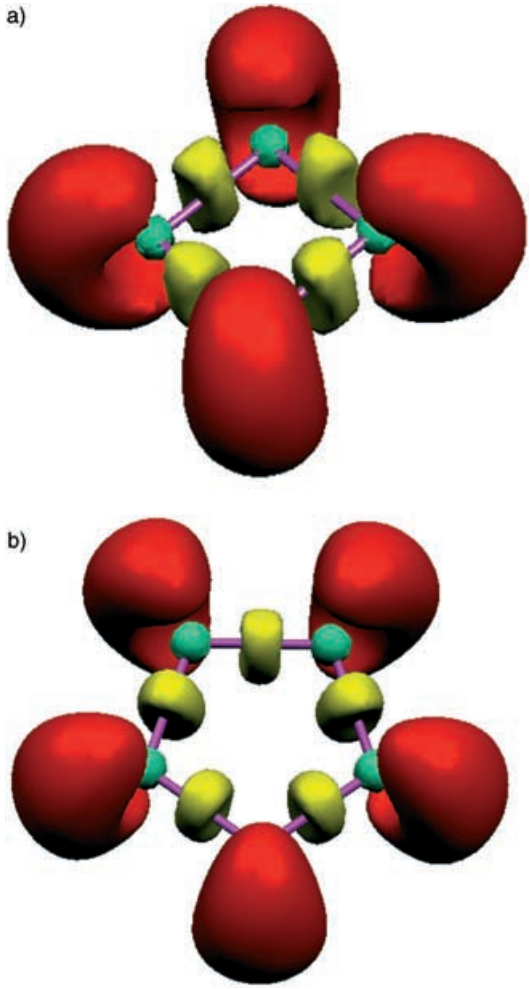

Figure 16. Projections of the ELF of P_4^{2-} (a) and P_5^- (b) with $\eta(r) = 0.78$. Core basins are color-coded turquoise, monosynaptic basins red, and disynaptic basins yellow.

Table 8. Population in electrons, population variance, and standard deviations of the ELF basins of the aromatic P_4^{2-} and comparison with hexaphosphane(8).

Basin[a]	Population	σ^2	σ
$C(P)$	10.06	0.43	0.66
$V(P)$	3.31	1.31	1.14
$V(P, P)$	2.10	1.13	1.06
scaled $V(P)$	1.55	1.32	1.15
scaled $V(P, P)$	1.11	1.06	1.03

[a] $C(P)$ is the mean core basin of the phosphorus atoms, and $V(P)$ denotes the mean monosynaptic valence basin. $V(P, P)$ is the mean disynaptic valence basin. "Scaled" refers to values obtained through division by the corresponding P_6H_8 values.

ecule (Table 8). The disynaptic valence basins in P_5^- show a similar trend with a population of 2.19 e and a variance of 1.15, just 1.16-fold more populated with a 1.07-fold higher variance than in P_6H_8 (Table 9). Thus, the P–P bonds in P_4^{2-} and P_5^- look more like the single bond in P_6H_8 and show no

Table 9. Population in electrons, population variance, and standard deviations of the ELF basins of the aromatic P_5^- and comparison with hexaphosphane(8).

Basin[a]	Population	σ^2	σ
$C(P)$	10.03	0.44	0.66
$V(P)$	2.96	1.	1.11
$V(P, P)$	2.19	1.15	1.07
scaled $V(P)$	1.38	1.24	1.11
scaled $V(P, P)$	1.16	1.07	1.04

[a] $C(P)$ is the mean core basin of the phosphorus atoms, and $V(P)$ denotes the mean monosynaptic valence basin. $V(P, P)$ is the mean disynaptic valence basin. "Scaled" refers to values obtained through division by the corresponding P_6H_8 values.

sign of the high electron delocalization found in benzene or the cyclopentadienide anion.

However, the monosynaptic valence basins of P_4^{2-} and P_5^- differ markedly from their P_6H_8 analogue. On the one hand, the shape of the lone pairs of P_4^{2-} and P_5^- is completely different from the lone pairs in P_6H_8, P_7^{3-}, P_{11}^{3-}, or P_4, as they are bent around the ring (Figure 16). On the other hand, the population of the monosynaptic valence basins is 3.31 e with a variance of 1.31 in P_4^{2-} and 2.96 e with a variance of 1. in P_5^-. Thus, P_4^{2-} shows a 1.55-fold more populated monosynaptic valence basin and a 1.32 times higher variance than the two central monosynaptic valence basins of P_6H_8. P_5^- shows a 1.38-fold higher population and a 1.24 times larger variance of its monosynaptic valence basins than in the reference compound. The same phenomenon is observed for the cyclotetrasulfur dication S_4^{2+} where the disynaptic (S–S) valence basins have a population of 1.81 e ($\sigma^2 = 1.03$), and the monosynaptic valence basins show a population of 3.63 e with a variance of 1.41, indicating the site of electron delocalization in this aromatic system. Additionally, calculations of the covariance matrix elements for the aromatic species P_4^{2-}, P_5^-, and S_4^{2+} show the contribution of the monosynaptic valence basins (lone pairs) to their variance to be higher in value than the contribution of the disynaptic valence basins to their variance, which confirms the delocalization.[75] For the nonaromatic molecules P_6H_8, P_4, P_7^{3-}, and P_{11}^{3-}, the situation is reversed.

In summary, the population and the variance of the monosynaptic and the disynaptic valence basins of P_7^{3-}, P_{11}^{3-}, and the reference species P_6H_8 are similar to each other, which indicates similar P–P single bonds and a similar lone pair character in all these species.

Since aromatic hydrocarbons have a high population and a high variance in the C–C bonds due to their aromaticity,[72] the aromatic P_4^{2-} and P_5^- should show the same behavior. However, the phosphorus–phosphorus bonds in P_4^{2-} and P_5^- are similar to those in P_6H_8, P_7^{3-}, and P_{11}^{3-}, which is unexpected. The high population and the high variance are found in the lone pairs of P_4^{2-} and P_5^-, indicating them to be the relevant electronic features for aromaticity in these species.

We conclude that the source and the phenomenology of aromaticity in P_4^{2-}, P_5^- and S_4^{2+}, viewed by the ELF

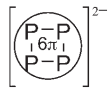

Figure 17. Structural formula of P_4^{2-}: the circle denotes the cyclic electron sextet on the outside of the phosphorus ring system.

method, differs from the aromaticity in aromatic hydrocarbons, and we propose the term "lone-pair aromaticity" for these heteroatom aromatic compounds (Figure 17).

Experimental Section

All the work was done with moisture and air excluded in an atmosphere of purified argon. Liquid ammonia was dried and stored over sodium metal. [18]Crown-6 was purified by sublimation.

NMR spectra were recorded with a variable temperature, multicore Avance Bruker spectrometer (^{1}H: 400 MHz). All ^{31}P spectra used liquid ammonia (300 μL) with [D_8]THF (100 μL) as solvent and were taken in the δ range +600 to −600 at −60 °C and −35 °C. The external references were phosphoric acid (85 %) for ^{31}P and TMS for ^{1}H spectra.

Synthesis of diphosphane(4): Diphosphane(4) was produced by hydrolyzing calcium phosphide in a modified apparatus according to Baudler.[35] All operations with diphosphane(4) are performed in a dark room using weak red light only.

Synthesis of Rb_3P_7: Rb_3P_7 was synthesized from distilled rubidium and electrograde red phosphorus according to the literature.[76]

Synthesis of M_4P_6 (M = K, Rb, Cs): Tantalum ampoules were charged with stoichiometric amounts of distilled metal and electrograde red phosphorus and were sealed under argon. Placed in evacuated Schlenk tubes, the ampoules were heated to 500 °C in tube furnaces for approximately 13 days.[31,33] The purity of the greenish-black powders was assayed by X-ray powder diffractometry (STADIP powder diffractometer (Stoe & Cie), $Cu_{K\alpha1}$ radiation, Ge single-crystal monochromator, Debye–Scherrer geometry, linear position-sensitive detector, Si as the external standard, indexing and refinement with the WinXPOW software).[77]

Ammonolysis of K_4P_6: Potassium phosphide(4/6) (100 mg) was dissolved in dry ammonia (10 mL). The blue solution became green, then finally yellow. A portion (about 500 μL) of this solution were transferred via a cooled capillary into a dry NMR tube and mixed with dry [D_8]THF (100 μL). ^{1}H NMR (400 MHz, NH_3, [D_8]THF, TMS ext., −60 °C): δ = −1.46 (d, ^1J(P,H) = 140 Hz, PH_2^-), 5.44 (s, NH_2^-), 6.46 (s, ?), 7.64 ppm (s, ?); ^{31}P{^{1}H} NMR (162 MHz, NH_3, [D_8]THF, H_3PO_4 ext., −60 °C): δ = 465.7 (s, P_5^-), 327.8 (s, P_4^{2-}), 175.0 (m, P_{11}^{3-}), −112.4 (m, P_{11}^{3-}), −4.4 (m, P_{11}^{3-}), −59.0 (m, P_7^{3-}), −110.0 (m, P_7^{3-}), −160.0 (m, P_7^{3-}), −21.3 (m, ?), −86.9 (m,?), −135.0 ppm (m,?).

Synthesis of $(K@[18]crown\text{-}6)_3K_3(P_7)_2\cdot 10NH_3$: Potassium phosphide(4/6) (100 mg; 0.29 mmol) and [18]crown-6 (310 mg: 1.17 mmol, 4 equiv) were placed in a flame-dried Schlenk tube and ammonia (15 mL) was condensed on the reagents. After seven days of storage at −40 °C, yellow, plate-shaped crystals were obtained which were subjected to low-temperature single-crystal X-ray analysis on a Stoe IPDS diffractometer (graphite monochromator, $Mo_{K\alpha}$ radiation, λ = 0.71073 Å). The structure was solved in space group $P\bar{1}$ with the SHELXS-97 program by direct methods.[78] After anisotropic refinement of the non-hydrogen atoms using SHELXL-97, an absorption correction was performed using DELrefABS from the PLATON program package.[79,80] Hydrogen atoms on crown ethers and on ammonia molecules coordinating with potassium ions were refined isotropically using a riding model. The hydrogen atoms on free ammonia molecules were located by Fourier cycling techniques and refined isotropically using restraints. After the refinement converged, a search for additional symmetry using PLATON and KPLOT had a negative result.[80,81] Crystallographic details are in Table 3. CCDC-266648 contains the supplementary crystallographic data for this paper. These data can be obtained free of charge from the Cambridge Crystallographic Data Centre via www.ccdc.cam.ac.uk/data_request/cif.

Synthesis of $Rb_3P_7\cdot 7NH_3$: Dry ammonia (10 mL) was distilled onto rubidium phosphide(3/7) (500 mg) in the reaction vessel at −78 °C. After storage at −40 °C for several weeks, yellow, plate-shaped crystals were formed which were analyzed on a Stoe IPDS diffractometer (graphite monochromator, $Mo_{K\alpha}$ radiation, λ = 0.71073 Å). The structure was solved with SHELXS-97 using direct methods in space group *Pbca*. After anisotropic refinement of the non-hydrogen atoms using SHELXL-97, an absorption correction was performed using DELrefABS from the PLATON program package.[79,80] Hydrogen atoms were located using Fourier cycling methods and refined isotropically with restraints employed. Crystallographic details are in Table 3. Further details of the crystal structure investigation are available from the Fachinformationszentrum Karlsruhe, 76344 Eggenstein-Leopoldshafen (Germany), (fax: (+49) 7247-808-666; e-mail: crysdata@fiz.karlsruhe.de) on quoting the depository number CSD 4158.

Synthesis of $(Rb@[18]crown\text{-}6)_3P_7\cdot 6NH_3$: A Schlenk tube was charged with rubidium phosphide(4/6) (100 mg; 0.19 mmol), [18]crown-6 (200 mg; 0.78 mmol), and dry liquid ammonia(10 mL). After three months' storage at −40 °C, yellow, needle-shaped crystals were obtained and subjected to X-ray single-crystal analysis on a Stoe IPDS diffractometer (graphite monochromator, $Mo_{K\alpha}$ radiation, λ = 0.71073 Å). The structure was solved in space group $P\bar{1}$ with the SHELXS-97 program using direct methods.[78] After anisotropic refinement of the non-hydrogen atoms using SHELXL-97, an absorption correction was performed using DELrefABS from the PLATON program package.[79,80] Hydrogen atoms on crown ethers and on ammonia molecules coordinating with rubidium ions were refined isotropically using a riding model. On some of the free ammonia molecules the hydrogen atoms were located by Fourier cycling techniques and refined isotropically using restraints. After the refinement converged, a search for additional symmetry using PLATON and KPLOT had negative results.[80,81] Crystallographic details are in Table 3. CCDC-266649 contains the supplementary crystallographic data for this paper. These data can be obtained free of charge from the Cambridge Crystallographic Data Centre via www.ccdc.cam.ac.uk/data_request/cif.

Synthesis of $Cs_2P_4\cdot 2NH_3$ using diphosphane(4): A Schlenk tube was charged with distilled cesium (1.1 g; 8.27 mmol), and diphosphane(4) (2 mL) was condensed into the tube at −78 °C. After the evolution of gas ceased, dry ammonia (10 mL) was condensed onto the product, yielding a yellow solution. After the reaction mixture had been stored at −40 °C for some days, yellow, cube-shaped crystals formed which were subjected to X-ray structure analysis on a Stoe IPDS diffractometer (graphite monochromator, $Mo_{K\alpha}$-radiation, λ = 0.71073 Å). The structure was solved with SHELXS-97 using direct methods in space group $P2_1/a$. After anisotropic refinement of the non-hydrogen atoms using SHELXL-97 an absorption correction was performed using DELrefABS from the PLATON program package.[79,80] Hydrogen atoms were located using Fourier cycling methods and refined isotropically. Crystallographic details are in Table 3. Further details of the crystal structure investigation are available from the Fachinformationszentrum Karlsruhe, 76344 Eggenstein-Leopoldshafen (Germany), (fax: (+49) 7247-808-666; e-mail: crysdata@fiz.karlsruhe.de) on quoting the depository number CSD 413072.

Synthesis of $Cs_2P_4\cdot 2NH_3$ using Cs_4P_6: Reaction of cesium phosphide(4/6) (100 mg) with liquid ammonia (10 mL) at −78 °C and storage for one month led to clean formation of $Cs_2P_4\cdot 2NH_3$ in the form of yellow, cube-shaped crystals, as evidenced by determination of the cell parameters of some of the crystals on the Stoe IPDS diffractometer. A portion (about 500 μL) of this solution was transferred via a cooled capillary to a dry NMR tube and mixed with dry [D_8]THF (100 μL). ^{1}H NMR (400 MHz, NH_3, [D_8]THF, TMS ext., −35 °C/−60 °C): δ = −1.43/−1.41 (d, ^1J(P,H) = 140 Hz, PH_2^-), 5.16/5.44 ppm (s, NH_2^-); ^{31}P{^{1}H} NMR (162 MHz, NH_3, [D_8]THF, H_3PO_4 ext., −35 °C/−60 °C): δ = 346.4/343.0 (s, P_4^{2-}), −269.2/−266.9 ppm (s, PH_2^-); ^{31}P NMR (162 MHz, NH_3, [D_8]THF, H_3PO_4 ext., −35 °C): δ = 346.4 (s, P_4^{2-}), −269.2 ppm (t, ^1J(P,H) = 140 Hz, PH_2^-).

Synthesis of $Cs_2P_4\cdot 2NH_3$ using the black reaction product of diphosphane(4) and ammonia: A Schlenk tube was charged with distilled cesium (1.26 g; 9.84 mmol), the black product (343 mg) of the P_2H_4–NH_3 reaction, and liquid ammonia (10 mL) at −78 °C. After storage at −40 °C for one month, orange, needle-shaped crystals of $Cs_3P_7\cdot 3NH_3$ and yellow,

cube-shaped crystals of $Cs_2P_4{\cdot}2NH_3$ were obtained, as evidenced by determination of the cell parameters of some of the crystals on the Stoe IPDS diffractometer. A portion (about 500 μL) of the solution was transferred via a cooled capillary into a dry NMR tube and mixed with dry [D$_8$]THF (100 μL). ^{1}H NMR (400 MHz, NH_3, [D$_8$]THF, TMS ext., −35 °C): $\delta = -1.46$ (d, ^1J(P,H) = 140 Hz, PH_2^-), −2.18 ppm (s, ?); ^{31}P{^{1}H} NMR (162 MHz, NH_3, [D$_8$]THF, H_3PO_4 ext., −35 °C): $\delta = 345.4$ (s, P_4^{2-}), −267.54 ppm (s, PH_2^-).

Theoretical procedures: All the geometries were optimized by the Gaussian03[82] package at the HF level of theory and 6-311++G(3df,3pd)[83–86] was applied as a basis set. To assure the usage of ground-state geometries in all calculations, the Hesse matrix was checked for the absence of imaginary entries.

The electron localization functions and basin populations were calculated with the ToPMoD package; a resolution of at least 0.1 Å was used throughout the calculations.[87,88]

For visualization, MOLEKEL 4.0[89] and MOLDEN[90] were used.

Acknowledgements

This work was supported by the Deutsche Forschungsgemeinschaft DFG and the Fonds der Chemischen Industrie. We thank Chemische Fabrik Wuelfel, Hannover, for generous amounts of calcium phosphide and zinc phosphide. F.K. thanks the Studienstiftung des Deutschen Volkes and the Fonds der Chemischen Industrie for a fellowship. We thank T. Hanauer for the preparation of larger amounts of polyphosphides and K. Pfisterer for the structure of $Rb_3P_7{\cdot}7NH_3$.

[1] J. A. N. F. Gomes, R. B. Mallion, *Chem. Rev.* **2001**, *101*, 1349–1383.
[2] R. V. Williams, *Chem. Rev.* **2001**, *101*, 1185–1204.
[3] K. Wade, *Adv. Inorg. Chem.* **1976**, *18*, 1–66.
[4] R. E. Williams, *Adv. Inorg. Chem.* **1976**, *18*, 67–142.
[5] E. Zintl, W. Dullenkopf, *Z. Physik. Chem.* **1932**, *B16*, 195–205.
[6] W. Klemm, *Proc. Chem. Soc. London* **1958**, 329–341.
[7] I. F. Hewaidy, E. Busmann, W. Klemm, *Z. Anorg. Allg. Chem.* **1964**, *328*, 283–293.
[8] E. Parthé, *Acta Crystallogr. Sect. B* **1973**, *29*, 2808–2815.
[9] E. Parthé, *Acta Crystallogr. Sect. B* **1980**, *36*, 1–7.
[10] R. J. Gillespie, J. Passmore, P. K. Ummat, O. C. Vaidya, *Inorg. Chem.* **1971**, *10*, 1327–1332.
[11] R. B. King, D. H. Rouvray, *J. Am. Chem. Soc.* **1977**, *99*, 7834–7840.
[12] R. B. King, *Chem. Rev.* **2001**, *101*, 1119–1152.
[13] M. Baudler, *Angew. Chem.* **1982**, *94*, 520–539; *Angew. Chem. Int. Ed. Engl.* **1982**, *21*, 492–512.
[14] M. Baudler, K. Glinka, *Chem. Rev.* **1993**, *93*, 16–1667.
[15] M. Baudler, K. Glinka, *Chem. Rev.* **1994**, *94*, 1273–1297.
[16] P. von Rague Schleyer, *J. Am. Chem. Soc.* **1958**, *80*, 1700–1704.
[17] G. Helmchen, G. Staiger, *Angew. Chem.* **1977**, *89*, 119–120; *Angew. Chem. Int. Ed. Engl.* **1977**, *16*, 116–117.
[18] D. Schroder, H. Schwarz, M. Wulf, H. Sievers, P. Jutzi, M. Reiher, *Angew. Chem.* **1999**, *111*, 37–3726; *Angew. Chem. Int. Ed.* **1999**, *38*, 3513–3515.
[19] S. Böcker, M. Häser, *Z. Anorg. Allg. Chem.* **1995**, *621*, 258–286.
[20] M. Häser, O. Treutler, *J. Chem. Phys.* **1995**, *102*, 3703–3711.
[21] M. Häser, U. Schneider, R. Ahlrichs, *J. Am. Chem. Soc.* **1992**, *114*, 9551–9559.
[22] P. Ballone, R. O. Jones, *J. Chem. Phys.* **1994**, *100*, 4941–4946.
[23] R. O. Jones, D. Hohl, *J. Chem. Phys.* **1990**, *92*, 6710–6721.
[24] R. Janoschek, *Chem.Ber.* **1992**, *125*, 2687–2689.
[25] R. O. Jones, G. Seifert, *J. Chem. Phys.* **1992**, *96*, 7564–7572.
[26] R. O. Jones, G. Ganteför, S. Hunsicker, P. Pieperhoff, *J. Chem. Phys.* **1995**, *103*, 9549–9562.
[27] G. Seifert, R. O. Jones, *J. Chem. Phys.* **1992**, *96*, 2951–2952.
[28] O. J. Scherer, J. Schwalb, M. Swarowsky, G. Wolmershauser, W. Kaim, R. Groß, *Chem. Ber.* **1988**, *121*, 443–449.
[29] M. Herberhold, G. Frohmader, W. Milius, *J. Organomet. Chem.* **1996**, *522*, 185–196.
[30] O. J. Scherer, H. Sitzmann, G. Wolmershauser, *Angew. Chem.* **1985**, *97*, 358–359; *Angew. Chem. Int. Ed. Engl.* **1985**, *24*, 351–353.
[31] H. P. Abicht, W. Hönle, H. G. von Schnering, *Z. Anorg. Allg. Chem.* **1984**, *519*, 7–.
[32] W. Schmettow, A. Lipka, H. G. von Schering, *Angew. Chem.* **1974**, *86*, 379–380; *Angew. Chem. Int. Ed. Engl.* **1974**, *13*, 345.
[33] H. G. von Schnering, T. Meyer, W. Hönle, W. Schmettow, U. Hinze, W. Bauhofer, G. Kliche, *Z. Anorg. Allg. Chem.* **1987**, *553*, 261–279.
[34] M. Baudler, S. Akpapoglou, D. Ouzounis, F. Wasgestian, B. Meinigke, H. Budzikiewicz, H. Münster, *Angew. Chem.* **1988**, *100*, 288–289; *Angew. Chem. Int. Ed. Engl.* **1988**, *27*, 280–281.
[35] M. Baudler, D. Düster, D. Ouzounis, *Z. Anorg. Allg. Chem.* **1987**, *544*, 87–94.
[36] M. Baudler, D. Ouzounis, *Z. Naturforsch. B: Chem. Sci.* **1989**, *44*, 381–382.
[37] M. Baudler, T. Etzbach, *Chem. Ber.* **1991**, *124*, 1159–1160.
[38] O. J. Scherer, T. Brück, *Angew. Chem.* **1987**, *99*, 59; *Angew. Chem. Int. Ed. Engl.* **1987**, *26*, 59.
[39] O. J. Scherer, J. Schwalb, G. Wolmershauser, W. Kaim, R. Groß, *Angew. Chem.* **1986**, *98*, 349–350; *Angew. Chem. Int. Ed. Engl.* **1986**, *25*, 363–364.
[40] J. Bai, A. V. Virovets, M. Scheer, *Science* **2003**, *300*, 781–783.
[41] F. Kraus, J. C. Aschenbrenner, N. Korber, *Angew. Chem.* **2003**, *115*, 4162–4165; *Angew. Chem. Int. Ed.* **2003**, *42*, 4030–4033.
[42] O. J. Scherer, *Nachr. Chem. Tech. Lab.* **1987**, *35*, 1140–1144.
[43] O. J. Scherer, J. Vondung, G. Wolmershauser, *Angew. Chem.* **1989**, *101*, 1395–1397; *Angew. Chem. Int. Ed. Engl.* **1989**, *28*, 1355–1357.
[44] M. Scheer, E. Herrmann, J. Sieler, M. Oehme, *Angew. Chem.* **1991**, *103*, 10–1025; *Angew. Chem. Int. Ed. Engl.* **1991**, *30*, 969–971.
[45] M. Scheer, C. Troitzsch, P. G. Jones, *Angew. Chem.* **1992**, *104*, 1395–1397; *Angew. Chem. Int. Ed. Engl.* **1992**, *31*, 1377–1379.
[46] M. Scheer, U. Becker, *Phosphorus, Sulfur Silicon Relat. Elem.* **1994**, *93–94*, 257–260.
[47] M. Scheer, K. Schuster, U. Becker, *Phosphorus, Sulfur Silicon Relat. Elem.* **1996**, *109–110*, 141–144.
[48] M. Scheer, U. Becker, *J. Organomet. Chem.* **1997**, *546*, 451–460.
[49] O. J. Scherer, *Acc. Chem. Res.* **1999**, *32*, 751–762.
[50] O. J. Scherer, *Angew. Chem.* **2000**, *112*, 1069–1071; *Angew. Chem. Int. Ed.* **2000**, *39*, 1029–1030.
[51] O. J. Scherer, *Chem. Unserer Zeit* **2000**, *34*, 374–381.
[52] O. J. Scherer, M. Swarowsky, G. Wolmershauser, *Angew. Chem.* **1988**, *100*, 4–424; *Angew. Chem. Int. Ed. Engl.* **1988**, *27*, 406.
[53] O. J. Scherer, M. Swarowsky, H. Swarowsky, G. Wolmershauser, *Angew. Chem.* **1988**, *100*, 738–739; *Angew. Chem. Int. Ed. Engl.* **1988**, *27*, 694–695.
[54] M. Baudler, C. Adamek, S. Opiela, H. Budzikiewicz, D. Ouzounis, *Angew. Chem.* **1988**, *100*, 1110–1111; *Angew. Chem. Int. Ed. Engl.* **1988**, *27*, 1059–1061.
[55] O. J. Scherer, T. Hilt, G. Wolmershauser, *Organometallics* **1998**, *17*, 4110–4112.
[56] L. Weber, U. Sonnenberg, *Chem. Ber.* **1991**, *124*, 725.
[57] M. Peruzzini, I. los Rios, A. Romerosa, F. Vizza, *Eur. J. Inorg. Chem.* **2001**, 593–608.
[58] M. Llunell, P. Alemany, S. Alvarez, V. P. Zhukov, A. Vernes, *Phys. Rev. B* **1996**, *53*, 10605–10609.
[59] W. Jeitschko, A. J. Foecker, D. Paschke, M. V. Dewalsky, C. B. H. Evers, B. Kuennen, A. Lang, G. Kotzyba, U. C. Rodewald, M. H. Moeller, *Z. Anorg. Allg. Chem.* **2000**, *626*, 1112–1120.
[60] E. H. Street, D. M. Gardner, C. E. Evers, *J. Am. Chem. Soc.* **1958**, *80*, 1819–1822.
[61] M. Baudler, P. Winzek, *Z. Anorg. Allg. Chem.* **1999**, *625*, 417–422.
[62] N. Korber, J. Daniels, *Helv. Chim. Acta* **1996**, *79*, 2083–2087.
[63] V. Manriquez, W. Hönle, H. G. von Schnering, *Z. Anorg. Allg. Chem.* **1986**, *539*, 95–109.
[64] J.Daniels, Dissertation thesis, Rheinische Friedrich-Wilhelms-Universität Bonn, **1998**.
[65] A. Fleischmann, Dissertation thesis, Universität Regensburg, **2002**.

[66] K. Pfisterer, Universität Regensburg, **1999**.
[67] J. C. Aschenbrenner, N. Korber, *Z. Anorg. Allg. Chem.* **2004**, *630*, 31–32.
[68] W. Hönle, H. G. von Schnering, *Z. Anorg. Allg. Chem.* **1978**, *440*, 171–182.
[69] T. Hanauer, M. Grothe, M. Reil, N. Korber, *Helv. Chim. Acta* **2005**, in press.
[70] H. M. Tuononen, R. Suontamo, J. Valkonen, R. S. Laitinen, *J. Phys. Chem. A* **2004**, *108*, 5670–5677.
[71] S. Noury, F. Colonna, A. Savin, B. Silvi, *J.Mol.Struct.* **1998**, *450*, 59–68.
[72] D. B. Chesnut, L. J. Bartolotti, *Chem. Phys.* **2000**, *253*, 1–11.
[73] A. D. Becke, K. E. J. Edgecombe, *J. Chem. Phys.* **1990**, *92*, 5397–5403.
[74] B. Silvi, A. Savin, *Nature* **1994**, *371*, 683–686.
[75] B. Silvi, *Phys. Chem. Chem. Phys.* **2004**, *6*, 256–260.
[76] H. G. von Schnering, W. Hönle, *Chem. Rev.* **1988**, *88*, 243–273.
[77] WinXPOW, version 1.08, STOE & Cie GmbH, Hilpertstrasse 10, 64295 Darmstadt (Germany), **2000**.
[78] G. M. Sheldrick, SHELXS-97, University of Göttingen, **1997**.
[79] G. M. Sheldrick, SHELXL-97, University of Göttingen, **1997**.
[80] A. L. Spek, PLATON—A Multipurpose Crystallographic Tool, Utrecht University, Utrecht, The Netherlands, **2003**..
[81] R. Hundt, KPLOT, version 8.7.10, University of Bonn, **2004**.
[82] M. J. Frisch, G. W.Trucks, H. B. Schlegel, G. E Scuseria, M. A. Robb, J. R. Cheeseman, , J. A. Montgomery Jr., T. Vreven, K. N. Kudin, J. C. Burant, J. M. Millam,S. S. Iyengar, J. Tomasi, V. Barone, B. Menucci, M. Cossi, G. Scalmani, N. Rega, G. A. Petersson, , H. Nakatsuji, M. Hada, , M. Ehara, , K. Toyota, R. Fukuda, J. Hasegawa, M. Ishida, T. Nakajima, Y. Honda, O. Kitao, H. Nakai, M. Klene, X. Li, J. E. Knox, H. P. Hratchian, J. B. Cross, C. Adamo, J. Jaramillo, R. Gomperts, R. E Stratmann, O. Yazyev, A. J. Austin, R. Cammi, C. Pomelli, J. Ochterski, P. Y. Ayala, K. Morokuma, G. A. Voth, P. Salvador, J. J. Dannenberg, V. G. Zakrzewski, S. Dapprich, A. D. Daniels, M. C. Strain, O. Farkas, A. D. Rabuck, K. Raghavachari, D. K. Malick, J. B. Foresman, J. V. Ortiz, Q. Cui, A. G. Baboul, S. Clifford, J. Cioslowski, B. B. Stefanov, G. Liu, A. Liashenko, P. Piskorz, I. Komaromi, R. L. Martin, D. J. Fox, T. Keith, M. A. Al-Laham,, C. Y. Peng, A. Nanayakkara, M. Challacombe, P. M. W. Gill, B. Johnson, W. Chen, M. W. Wong, C. Gonzalez, J. A. Pople, Gaussian 03, version B.04, Gaussian, Inc., Pittsburgh PA, **2003**.
[83] R. Krishnan, J. S. Binkley, R. Seeger, J. A. Pople, *Chem. Phys. Lett.* **1980**, *72*, 650.
[84] A. D. McLean, G. S. Chandler, *J. Chem. Phys.* **1980**, *72*, 5639.
[85] T. Clark, J. Chandrasekhar, G. W. Spitznagel, P. von R. Schleyer, *J. Comput. Chem.* **1983**, *4*, 294.
[86] M. J. Frisch, J. A. Pople, J. S. Binkley, *J. Chem. Phys.* **1984**, *80*, 3265.
[87] S. Noury, X. Krokidis, F. Fuster, B. Silvi, ToPMoD, Laboratoire de Chimie Théorique (UMR-CNRS 7616), Université Pierre et Marie Curie, 75252 Paris cédex, France, **1997**.
[88] S. Noury, X. Krokidis, F. Fuster, B. Silvi, *Comput. Chem.* **1999**, 597–604.
[89] P. Flükinger, H. P. Lüthi, S. Portmann, J. Weber, MOLEKEL, version 4.0, Manno (Switzerland), Swiss Center for Scientific Computing, **2000**.
[90] G. Schaftenaar, J. H. Noordik, *J. Comput.-Aided Mol. Des.* **2000**, *14*, 1–134.

Received: April 13, 2005
Published online: July 29, 2005

